Acta Crystallographica Section A
Foundations of Crystallography
ISSN 0108-7673

Received 25 October 2011
Accepted 28 December 2011

Lattice refinement strategies

John K. Edmiston,[a,b]* Joel V. Bernier,[b] Nathan R. Barton[b] and George C. Johnson[a]

[a]University of California, Berkeley, USA, and [b]Lawrence Livermore National Laboratory, Livermore, USA. Correspondence e-mail: jedmiston@berkeley.edu

This article quantitatively reconciles crystallographic and mechanics approaches to lattice refinement as part of X-ray diffraction procedures. The equivalence between the refinement based on unit-cell parameters to that based on a lattice deformation tensor is established from a fixed reference configuration. Justification for the small strain assumption, commonly employed in X-ray diffraction based stress analysis, is also derived. It is shown that relations based on infinitesimal strains are correct to within an error of quadratic order in strain. This error may be important to consider for high-precision or high-strain experiments. It is hoped that these results are of use for facilitating communication and collaboration between crystallography and experimental mechanics communities, for studies where X-ray diffraction data are the fundamental measurement.

1. Introduction

The increased use of X-ray diffraction experiments in support of mechanics of materials studies (Winther *et al.*, 2004; Mach *et al.*, 2010; Efstathiou *et al.*, 2010) has led to increased overlap between the communities of applied crystallography and mechanics. Interactions among members of the community suggest that there may be some benefit in relating certain viewpoints native to crystallographers to those from a mechanics background. For example, crystallographers typically consider the procedure of lattice refinement in terms of unit-cell parameters and grain orientation, whereas mechanicians fix an appropriately chosen reference configuration to the material, denoted by κ, and resolve the linear transformation from the reference configuration to the current state. This transformation is denoted by $\boldsymbol{H}_\kappa$[1] and will be referred to as the lattice deformation tensor. The fixed reference configuration approach is convenient to use for determining elastic stresses, since in phenomenological continuum theories constitutive formulas are described in terms of functions of $\boldsymbol{H}_\kappa$ (Chadwick, 1999; Liu, 2002). Establishing the mathematical equivalences and pointing out subtle differences between these two approaches is one outcome of this article.

It is noteworthy that both methods of describing lattice deformation are capable of characterizing finite strains. Therefore, as a related topic we take this opportunity to address the formal relationship between measures of finite strains and measures of infinitesimal strains, the latter of which are typically used in mechanics studies (Cullity, 1978; Noyan & Cohen, 1987; Miller *et al.*, 2008). By infinitesimal strains we mean the use of formulas analogous in philosophy to

$$\varepsilon(\mathbf{N}) = \delta d/d_0, \tag{1}$$

where ε is a scalar strain measure, $\mathbf{N}$ denotes the normal to the lattice plane under consideration, and $\delta d = d_\mathrm{f} - d_0$, where d_0 and d_f are the initial and deformed planar spacings, respectively. The planar spacing, d, is related to the diffraction angle, θ, by Bragg's law, $2d\sin\theta = n\lambda$, where λ is the wavelength. Equation (1) along with Bragg's law thereby forms a framework in which the infinitesimal strain tensor $\boldsymbol{\varepsilon}$ may be estimated from the evolution of diffraction peak shifts $\delta\theta$ (Cullity, 1978).

Most crystalline materials yield before reaching the levels of distortion which would make infinitesimal strain measures unacceptably erroneous compared with a finite deformation measure such as $\boldsymbol{H}_\kappa$. However, recent experiments are pushing this envelope. Large elastic strains are possible for short-timescale studies such as impact loading, where plastic flow is absent (Kalantar *et al.*, 2005; Hawreliak *et al.*, 2011), or when high hydrostatic pressures are imposed, such as those attained in diamond anvil cell experiments (Jayaraman, 1983; Yamanaka *et al.*, 2001; Katrusiak, 2008). Although to date the error in using infinitesimal kinematic[2] measures has been acceptable, since typically $|\varepsilon| < 1\%$, finite deformation measures may become important to consider as experimental techniques enable large-strain studies. Similarly, as higher experimental resolutions are attained, these issues may be important to consider, since precision is brought into a regime where large-strain details are significant.

We present this study in two primary sections. In §2 we relate the approaches to lattice refinement based on unit-cell parameters to that based on a fixed reference configuration.

[1] In the phenomenological plasticity literature, $\boldsymbol{H}_\kappa$ is also commonly referred to as $\boldsymbol{F}^\mathrm{e}$. The choice of designation $\boldsymbol{H}_\kappa$ follows the conventions of Gupta *et al.* (2011).

[2] In this article the term kinematic will be used to connote the idea of motion or deformation, as opposed to its definition with respect to the kinematic theory of X-ray diffraction.

We give the mathematical system of equations which may be solved to relate one set of refinement parameters to the other. Then in §3 we describe the application of the fixed reference approach to X-ray diffraction data by arriving at an equation which expresses the evolution of reciprocal-lattice vectors under finite lattice deformations. Using this result we are able to quantify the error made in using infinitesimal kinematic relations by computing the leading order in strain expansion of the finite deformation description.

2. Comparison of lattice refinement procedures

The primary outcome of many X-ray diffraction experiments is to determine the state of lattice deformation in individual crystal grains. For these studies, lattice refinement refers to the stage of analysis where initial orientations have been determined by an indexing method, but where more precise information about the lattice state is sought. As noted in the *Introduction*, the approaches taken for this procedure differ between crystallography and mechanics researchers, although both are capable of describing finite strains. In this section we will show how these methods of lattice refinement are related to one another, and highlight potential aspects to consider when using one framework or the other.

In overview, the typical methodology for crystallographers would be to view lattice refinement as the determination of the unit-cell parameters (six parameters), along with an orientation of the crystal (three parameters), for a total of nine parameters. A mechanician would approach the same problem by determining the lattice deformation tensor from a fixed reference configuration (nine components). For example, the fixed reference configuration may be generated by fixed unit-cell parameters at a convenient state, typically the ambient unstressed state of the crystal.

For simple lattices we can explicitly link the two approaches. The extension to non-simple lattices is straightforward and the required computations are evident from the analysis to follow. For another perspective, see the review by Adams & Olson (1998).

2.1. Interpretation of the unit-cell approach

To explicitly compare the two methods of lattice refinement under consideration we require a common point of reference; for this we find it easier to translate the unit-cell approach into the fixed reference language. To achieve this we first consider a reference cube aligned with a Cartesian basis $\mathbf{e}_1, \mathbf{e}_2, \mathbf{e}_3$. For later use, the reciprocal vectors in this configuration are trivial owing to orthonormality of the Cartesian system; we have

$$\mathbf{e}_1^* = \mathbf{e}_1, \quad \mathbf{e}_2^* = \mathbf{e}_2, \quad \mathbf{e}_3^* = \mathbf{e}_3, \tag{2}$$

where $\mathbf{e}_i^*$, $i = 1, 2, 3$, are the reciprocal basis vectors to $\mathbf{e}_i$. Throughout this article, reciprocal vectors will be distinguished by the notation $(\cdot)^*$. Next, the reference cube is deformed by a structural map, *e.g.* a linear transformation $\boldsymbol{H}_s$, which takes the reference cube into its configuration where unit-cell parameters are conventionally defined (see Fig. 1).

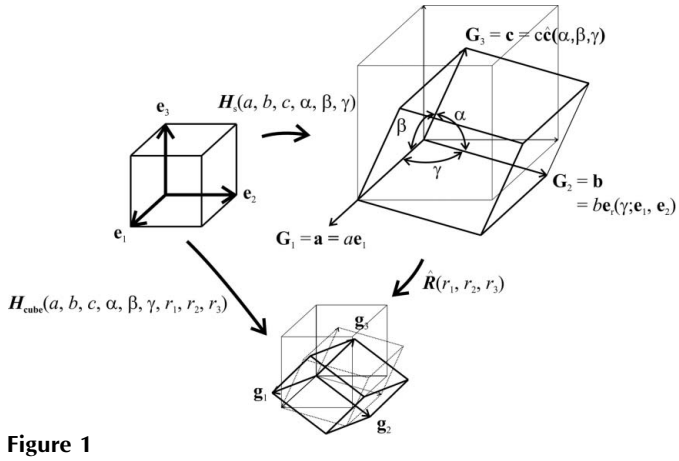

Figure 1
Depiction of the lattice refinement procedure using six unit-cell parameters and three rotation parameters to arrive at the physical configuration of the crystal where diffraction is measured. The final state based on evolution from the initial cube is given by the mapping $\boldsymbol{H}_{\text{cube}} = \hat{\boldsymbol{R}}\boldsymbol{H}_s$.

Now consider the evolution of the cube axes $\mathbf{e}_1, \mathbf{e}_2, \mathbf{e}_3$ under the action of the structural map, $\boldsymbol{H}_s$. The new configuration is defined by the three length changes of the cube axes, a, b, c, and the internal angles of the cell edges, α, β, γ (Callister, 2000). We construct this deformation according to the following definitions,

$$\boldsymbol{H}_s\mathbf{e}_1 \equiv \mathbf{a} = a\mathbf{e}_1, \tag{3}$$

$$\boldsymbol{H}_s\mathbf{e}_2 \equiv \mathbf{b} = b\mathbf{e}_r(\gamma; \mathbf{e}_1, \mathbf{e}_2), \tag{4}$$

$$\boldsymbol{H}_s\mathbf{e}_3 \equiv \mathbf{c} = c\hat{\mathbf{c}}(\alpha, \beta, \gamma), \tag{5}$$

where $\mathbf{a}, \mathbf{b}, \mathbf{c}$ are the unit-cell edges after the structural map, and where we are using the assignment of the polar coordinate unit vector $\mathbf{e}_r$ defined by

$$\mathbf{e}_r(\gamma; \mathbf{e}_1, \mathbf{e}_2) = \cos\gamma\mathbf{e}_1 + \sin\gamma\mathbf{e}_2. \tag{6}$$

In (5) we are using $\hat{\mathbf{c}} = \mathbf{c}/|\mathbf{c}|$ to denote the unitization operation. This notation will be used again later in this article. The Cartesian representation for $\mathbf{c}$, which is defined off the internal angles α, β, γ, is lengthy to compute; details are provided in Appendix *A* [see equation (54)]. Also consult Neustadt *et al.* (1968) for an alternative point of view on this computation. The relations defining the structural map in equations (3)–(5) have a generalized interpretation, commonly encountered in mechanics, which encodes any convective mapping between configurations. To show this, we first assign a basis to a reference configuration $\mathbf{G}_i$, $i = 1, 2, 3$, where $\mathbf{G}_i$ are, here, interpreted as being fixed to the lattice, *e.g.* they are (direct) lattice vectors. Corresponding to $\mathbf{G}_i$ we can compute the reciprocal basis $\mathbf{G}_i^*$, $i = 1, 2, 3$, with the property

$$\mathbf{G}_i \cdot \mathbf{G}_j^* = \delta_{ij}. \tag{7}$$

Under a deformation by $\boldsymbol{H}$, the mapped basis, $\mathbf{g}_i$, is defined by

$$\mathbf{g}_i = \boldsymbol{H}\mathbf{G}_i, \quad i = 1, 2, 3. \tag{8}$$

Therefore, by inspection, we can use (8) with (7) to deduce that $\boldsymbol{H}$ has the representation

$$\boldsymbol{H} = \mathbf{g}_i \otimes \mathbf{G}_i^*, \tag{9}$$

with repeated indices indicating the summation convention is in effect, here and for the rest of the article. The tensor product $\otimes$ is defined operationally by $(\mathbf{q} \otimes \mathbf{r})\mathbf{s} \equiv \mathbf{q}(\mathbf{r} \cdot \mathbf{s})$ for vectors $\mathbf{q}, \mathbf{r}, \mathbf{s}$. To demonstrate (9), consider the sequence $\boldsymbol{H}\mathbf{G}_j = (\mathbf{g}_i \otimes \mathbf{G}_i^*)\mathbf{G}_j = \mathbf{g}_i\delta_{ij} = \mathbf{g}_j$, in which we have used (7).

Now returning to the consideration of equations (3)–(5), recall that equation (2) defines the reciprocal basis $\mathbf{G}_i^*$ ($\equiv \mathbf{e}_i^*$) with respect to the reference cube configuration. Then we can apply (9) and (8) to (3)–(5), observe that $\mathbf{a} \equiv \mathbf{g}_1$, $\mathbf{b} \equiv \mathbf{g}_2$ and $\mathbf{c} \equiv \mathbf{g}_3$, and see that $\boldsymbol{H}_\mathrm{s}$ has the representation

$$\begin{aligned}\boldsymbol{H}_\mathrm{s} &= \mathbf{a} \otimes \mathbf{e}_1 + \mathbf{b} \otimes \mathbf{e}_2 + \mathbf{c} \otimes \mathbf{e}_3 \\ &= a\mathbf{e}_1 \otimes \mathbf{e}_1 + b\mathbf{e}_r(\alpha; \mathbf{e}_1, \mathbf{e}_2) \otimes \mathbf{e}_2 + c\hat{\mathbf{c}}(\alpha, \beta, \gamma) \otimes \mathbf{e}_3. \end{aligned} \tag{10}$$

As an example we display equation (10) in matrix form for the general triclinic case. Resolving on the Cartesian basis $\{\mathbf{e}_i\}$ gives

$$\boldsymbol{H}_\mathrm{s} = \begin{bmatrix} a & b\cos\gamma & c\cos\beta \\ 0 & b\sin\gamma & c(\cos\alpha - \cos\beta\cos\gamma)/\sin\gamma \\ 0 & 0 & c(1 + 2\cos\alpha\cos\beta\cos\gamma - \cos^2\alpha - \cos^2\beta - \cos^2\gamma)^{1/2}/\sin\gamma \end{bmatrix}_{\mathbf{e}_i \otimes \mathbf{e}_j} \tag{11}$$

where $\mathbf{e}_i \otimes \mathbf{e}_j$ denotes the tensorial basis being used. Details of the computations leading to (11) are provided in Appendix *A*.

So far we have only related unit-cell parameters to the structural map of a convenient artificial reference cube. To complete the lattice refinement problem we must be able to account for the orientation of the physical configuration of the lattice when the X-ray observation is made. In the mechanics literature the physical configuration is also called the current configuration; this usage will prevail in the rest of this article. Therefore, to go from the structural map configuration to an arbitrary current configuration, an additional rotation operation, denoted by $\hat{\boldsymbol{R}} \in O(3, \mathbb{R})$, is required. This rotation tensor may be parametrized by three coordinates, *e.g.* Euler angles or angle axis parameters. Finally, the full set of parameters characterizing the deformation from the reference cube to the current configuration are summarized by

$$\begin{aligned}\boldsymbol{H}_\mathrm{cube}(r_1, r_2, r_3, a, b, c, \alpha, \beta, \gamma) = \\ \hat{\boldsymbol{R}}(r_1, r_2, r_3)\boldsymbol{H}_\mathrm{s}(a, b, c, \alpha, \beta, \gamma),\end{aligned} \tag{12}$$

where r_1, r_2, r_3 are, for example, the angle axis parameters for a rotation. The lattice refinement procedure then occurs on the array $r_1, r_2, r_3, a, b, c, \alpha, \beta, \gamma$; that is, these values are modified to match experimental diffraction data *via* an algorithm such as least squares. The entire process is depicted in Fig. 1, where the actions of the structural map $\boldsymbol{H}_\mathrm{s}$ and rotation $\hat{\boldsymbol{R}}$ are illustrated, arriving at the final configuration where the diffraction measurement is made.

2.2. Mechanistic approach

In this approach the same problem of lattice refinement is accomplished in a slightly different way, by first fixing the lattice parameters at a natural reference state, *e.g.* assign a_0, b_0, c_0, α_0, β_0, γ_0. Using (10), these parameters then generate a fixed structural map of the cube, denoted $\boldsymbol{H}_{\mathrm{s},0}$. The result of the action of $\boldsymbol{H}_{\mathrm{s},0}$ on the cube defines what is referred to as the reference configuration, denoted κ. The parameters a_0, b_0, c_0, α_0, β_0, γ_0 are usually obtained from experiments performed when the material is in its ambient stress-free state. Then, with an eye toward constitutive equations, stresses are naturally determined by deformations of the lattice from this fixed reference state. Deformation tensors from the reference κ are denoted by $\boldsymbol{H}_\kappa$ to emphasize the dependence on the configuration κ. For physical processes, $\boldsymbol{H}_\kappa$ will be invertible, so that the polar decomposition theorem applies. Thus there is an orthogonal tensor $\boldsymbol{R}$ and a symmetric, positive definite stretch tensor $\boldsymbol{U}$ such that

$$\boldsymbol{H}_\kappa = \boldsymbol{R}\boldsymbol{U}. \tag{13}$$

The orthogonal tensor $\boldsymbol{R}$ accounts for the rotation of the lattice, and the stretch tensor $\boldsymbol{U}$ represents lattice distortion. Looking ahead, in §3 more details will be given showing how $\boldsymbol{U}$ is related to the infinitesimal strain tensor $\boldsymbol{\varepsilon}$. For example, one aspect they differ in is that, in an ambient state, $\boldsymbol{U} = \boldsymbol{I}$, while, in the same state, $\boldsymbol{\varepsilon} = 0$. Instead of equation (13) we could also have the equivalent formulation $\boldsymbol{H}_\kappa = \boldsymbol{V}\boldsymbol{R}$, where $\boldsymbol{V} = \boldsymbol{R}\boldsymbol{U}\boldsymbol{R}^\mathrm{T}$. See Bernier *et al.* (2011) for further discussion and crystallographic considerations of employing the right ($\boldsymbol{R}\boldsymbol{U}$) or left ($\boldsymbol{V}\boldsymbol{R}$) decomposition in algorithms. The map from the fixed reference configuration, κ, to the current configuration may then be written as

$$\begin{aligned}\boldsymbol{H}_\kappa(r_1, r_2, r_3, U_{11}, U_{22}, U_{33}, U_{23}, U_{13}, U_{12}) = \\ \boldsymbol{R}(r_1, r_2, r_3)\boldsymbol{U}(U_{11}, U_{22}, U_{33}, U_{23}, U_{13}, U_{12}),\end{aligned} \tag{14}$$

where $\boldsymbol{R}$ is parametrized by three coordinates, and the stretch tensor is parametrized by six coordinates owing to symmetry, $\boldsymbol{U} = \boldsymbol{U}^\mathrm{T}$. Lattice refinement then occurs on the array $r_1, r_2, r_3, U_{11}, U_{22}, U_{33}, U_{23}, U_{13}, U_{12}$. The entire process, starting from

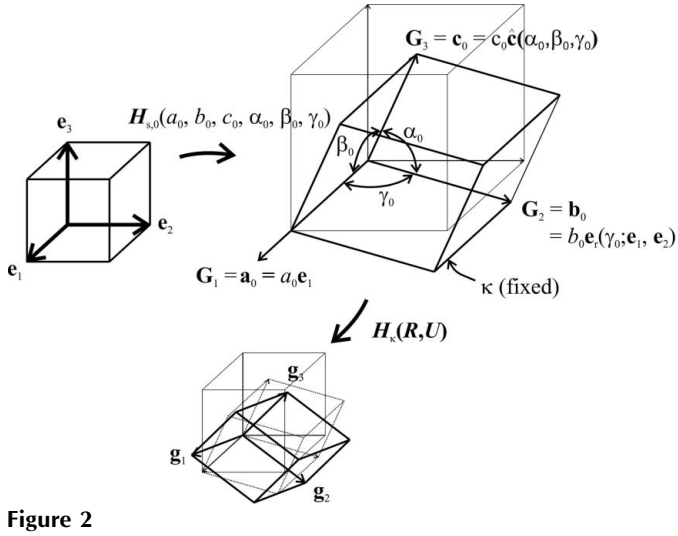

Figure 2
Depiction of the lattice refinement procedure based on evolution from a fixed reference configuration, κ. The initial structural map $\boldsymbol{H}_{\mathrm{s},0}$ is fixed and lattice refinement consists of obtaining the nine components of a deformation tensor from the reference state, $\boldsymbol{H}_\kappa$. The final state based on evolution from the initial cube is given by the mapping $\boldsymbol{H}_\mathrm{cube} = \boldsymbol{H}_\kappa\boldsymbol{H}_{\mathrm{s},0}$.

the initial cube, is shown in Fig. 2, which shows the action of the fixed reference structural map $\boldsymbol{H}_{s,0}$, followed by $\boldsymbol{H}_\kappa$ to achieve the final state.

2.3. Comparison of crystallographic and mechanistic approaches

The approaches so far described (unit cells, fixed reference) can now be related to one another by considering the mappings from the initial cube to the final state. Since such mappings must agree on the geometry of the lattice in the final configuration, either approach should give the same result. Therefore we have the relation

$$\boldsymbol{H}_{\rm cube} = \boldsymbol{H}_\kappa \boldsymbol{H}_{s,0} = \hat{\boldsymbol{R}} \boldsymbol{H}_s. \tag{15}$$

The equivalence is illustrated graphically by comparing Figs. 1 and 2. To more explicitly demonstrate, let us assume we are given $(\boldsymbol{H}_s, \hat{\boldsymbol{R}})$ from fitting the unit-cell parameters and rotation. Recall we are using equation (11) to generate $\boldsymbol{H}_s$ from the unit-cell parameters. Then we can use (15) to compute $\boldsymbol{H}_\kappa = \hat{\boldsymbol{R}} \boldsymbol{H}_s \boldsymbol{H}_{s,0}^{-1}$, and thereby obtain the lattice deformation tensor. The solution to the polar decomposition problem for rotation and stretch factors of $\boldsymbol{H}_\kappa$ can be computed by a variety of methods which we do not discuss here [see Liu (2002), p. 6, for an example]. Conversely, given $\boldsymbol{H}_\kappa, \boldsymbol{H}_{s,0}$, we can solve for the lattice parameters by manipulating (15) and performing the required vector projections on (10),

$$\mathbf{a} \cdot \mathbf{e}_1 = a = \boldsymbol{H}_s \mathbf{e}_1 \cdot \mathbf{e}_1 = \hat{\boldsymbol{R}}^{\rm T} \boldsymbol{H}_\kappa \boldsymbol{H}_{s,0} \mathbf{e}_1 \cdot \mathbf{e}_1, \tag{16}$$

$$\mathbf{b} \cdot \mathbf{e}_1 = b \cos\alpha = \boldsymbol{H}_s \mathbf{e}_2 \cdot \mathbf{e}_1 = \hat{\boldsymbol{R}}^{\rm T} \boldsymbol{H}_\kappa \boldsymbol{H}_{s,0} \mathbf{e}_2 \cdot \mathbf{e}_1, \tag{17}$$

$$\mathbf{b} \cdot \mathbf{e}_2 = b \sin\alpha = \boldsymbol{H}_s \mathbf{e}_2 \cdot \mathbf{e}_2 = \hat{\boldsymbol{R}}^{\rm T} \boldsymbol{H}_\kappa \boldsymbol{H}_{s,0} \mathbf{e}_2 \cdot \mathbf{e}_2, \tag{18}$$

$$\mathbf{c} \cdot \mathbf{e}_1 = c \cos\beta = \boldsymbol{H}_s \mathbf{e}_3 \cdot \mathbf{e}_1 = \hat{\boldsymbol{R}}^{\rm T} \boldsymbol{H}_\kappa \boldsymbol{H}_{s,0} \mathbf{e}_3 \cdot \mathbf{e}_1, \tag{19}$$

$$\mathbf{c} \cdot \mathbf{e}_2 = \boldsymbol{H}_s \mathbf{e}_3 \cdot \mathbf{e}_2 = \hat{\boldsymbol{R}}^{\rm T} \boldsymbol{H}_\kappa \boldsymbol{H}_{s,0} \mathbf{e}_3 \cdot \mathbf{e}_2, \tag{20}$$

$$\mathbf{c} \cdot \mathbf{e}_3 = \boldsymbol{H}_s \mathbf{e}_3 \cdot \mathbf{e}_3 = \hat{\boldsymbol{R}}^{\rm T} \boldsymbol{H}_\kappa \boldsymbol{H}_{s,0} \mathbf{e}_3 \cdot \mathbf{e}_3. \tag{21}$$

In (20) and (21) we have omitted the expressions for $\mathbf{c} \cdot \mathbf{e}_2$, $\mathbf{c} \cdot \mathbf{e}_3$ for reasons of appearance; these terms are recorded in the $i, j = (2, 3), (3, 3)$ components of the matrix representation of $\boldsymbol{H}_s$ in (11). The system of equations (16)–(21) can then be solved for $a, b, c, \alpha, \beta, \gamma$ in terms of $\boldsymbol{H}_\kappa, \hat{\boldsymbol{R}}, \boldsymbol{H}_{s,0}$. Some assistance in solving equations (17)–(21) comes from employing relations like

$$b = |\mathbf{b}| = (\boldsymbol{H}_s \mathbf{e}_2 \cdot \boldsymbol{H}_s \mathbf{e}_2)^{1/2}, \tag{22}$$

$$c = |\mathbf{c}| = (\boldsymbol{H}_s \mathbf{e}_3 \cdot \boldsymbol{H}_s \mathbf{e}_3)^{1/2}. \tag{23}$$

Therefore we have shown that the results of a refinement by one method can be used to solve for the other set of parameters. However, there are some subtle distinctions we now discuss. Noting the polar decomposition theorem, equation (13), and examining equation (12), we can see that adjusting the lattice parameters $a, b, c, \alpha, \beta, \gamma$ induces elements of both stretch and rotation, since $\boldsymbol{H}_s$ is not generally symmetric, see equation (11). This is important to note because it can be shown that stresses arise only due to stretching through $\boldsymbol{U}$, and not due to rigid-body rotations (Chadwick, 1999). Therefore there can be some quantitative differences in the results of the two approaches, particularly when considering uncertainty analysis in stress studies (Edmiston *et al.*, 2011).

In any case, hopefully this discussion is useful for facilitating communication and joint activity between crystallography and mechanics communities in the future.

It is important to recognize that methods using unit-cell parameters or deformation tensors to describe the lattice state are each capable of accurately quantifying large strain kinematics. In many studies, however, it has been common to use infinitesimal strain tensors, $\boldsymbol{\varepsilon}$, to describe lattice distortion. In the next section we use the fixed reference description of lattice deformations to quantify the error made in using infinitesimal kinematics along the lines of equation (1). To do this we first derive a relation for the evolution of reciprocal-lattice vectors which is analogous to equation (8) for lattice vectors. This relation should be useful for implementing lattice refinement procedures using the finite deformation measures $\boldsymbol{H}_\kappa$ into X-ray diffraction analysis codes.

3. Error in small strain estimate

3.1. Reciprocal vector kinematics

To obtain the error in the small strain estimate we first derive an expression for the evolution of reciprocal-lattice vectors under finite lattice deformations, $\boldsymbol{H}$. Here and for the rest of this section, we suppress the explicit designation of the reference configuration κ from quantities such as $\boldsymbol{H}_\kappa$ for convenience. The reciprocal-lattice construction arising from the classical theory of X-ray diffraction is convenient and powerful (Guiner, 1963; Azaroff *et al.*, 1974; Cullity, 1978). Using this, we can analyze X-ray diffraction patterns of strained crystals by simply considering geometric aspects of the reciprocal-lattice vectors. We now work out the details.

Recall that equation (8) relates lattice vectors in a deformed and reference configuration, $\mathbf{g}_i$ and $\mathbf{G}_i$, respectively, through the action of $\boldsymbol{H}$. We can derive an analogous relation for deformed and reference reciprocal-lattice vectors, without introducing formal notions of differential geometry as follows. Denote $\mathbf{g}_i^*$, $\mathbf{G}_i^*$ to be the reciprocal vector basis corresponding to $\mathbf{g}_i$, $\mathbf{G}_i$, respectively. Note that the identity $\boldsymbol{I}$ may be written

$$\boldsymbol{I} = \mathbf{g}_i \otimes \mathbf{G}_i^* = \mathbf{g}_i \otimes \mathbf{g}_i^*. \tag{24}$$

This is evident by observing that, for example, $\boldsymbol{I}\mathbf{G}_i = \mathbf{G}_i$, and noting the requirement between direct and reciprocal vectors, equation (7). With equation (24), the definition of the inverse deformation $\boldsymbol{H}^{-1}$ as $\boldsymbol{H}\boldsymbol{H}^{-1} = \boldsymbol{I}$, and with $\boldsymbol{H}$ represented by equation (9), we have, by inspection,

$$\boldsymbol{H}^{-1} = \mathbf{G}_i \otimes \mathbf{g}_i^*. \tag{25}$$

We can then compute the transpose of $\boldsymbol{H}^{-1}$ easily from equation (25), giving

$$\boldsymbol{H}^{-\mathrm{T}} = \mathbf{g}_i^* \otimes \mathbf{G}_i. \tag{26}$$

Therefore, we have the useful result

$$\boldsymbol{H}^{-\mathrm{T}}\mathbf{G}_i^* = \mathbf{g}_i^*. \tag{27}$$

To see this, consider the sequence $\boldsymbol{H}^{-\mathrm{T}}\mathbf{G}_i^* = (\mathbf{g}_j^* \otimes \mathbf{G}_j)\mathbf{G}_i^* = \mathbf{g}_j^*\delta_{ij} = \mathbf{g}_i^*$, where we have used equation (7). This result is analogous to equation (8), but here we describe the evolution of reciprocal vectors under deformation, rather than that of lattice vectors.

Noting the arbitrariness of the choice of the reference lattice vectors $\mathbf{G}_i$ which began the derivations (*i.e.* there are many equivalent unit cells which generate the same crystal lattice), we can conclude that

$$\boldsymbol{H}^{-\mathrm{T}}\mathbf{G}_{(i)}^* = \mathbf{g}_{(i)}^* \tag{28}$$

holds for any associated reference and deformed reciprocal vectors $\mathbf{G}_{(i)}^*$, $\mathbf{g}_{(i)}^*$. Here (i) is a bookkeeping index into the set of all reciprocal-lattice vectors. For example, by enumerating the *hkl* indices, we assign $\mathbf{G}_{(i)}^*$ to correspond to the ith *hkl* value. Equation (28) thus forms the foundation for generating residuals in a least-squares implementation, whose solution gives a best-fit estimate of the grain-averaged finite deformation tensor $\boldsymbol{H}$. For further details this was carried out on experimental data by Edmiston *et al.* (2011).

We now consider the typical expressions used for infinitesimal strain analysis in the literature, which differ in appearance from equation (28). Common methodologies for strain analysis take fundamental relation

$$\boldsymbol{\varepsilon} \cdot \mathbf{N}^{(i)} \otimes \mathbf{N}^{(i)} = \delta d^{(i)}/d_0^{(i)}, \tag{29}$$

where $||\boldsymbol{\varepsilon}|| \ll 1$ is the infinitesimal strain tensor, $\mathbf{N}^{(i)}$ is the normal vector to the ith lattice plane, and $\delta d^{(i)} \equiv d_{\mathrm{f}}^{(i)} - d_0^{(i)}$ is the change in planar spacing for the ith reflection. Here $d_{\mathrm{f}}^{(i)}$ is the deformed spacing and $d_0^{(i)}$ is the initial spacing. In (29) the inner product on tensors is defined operationally by $\boldsymbol{\varepsilon} \cdot \mathbf{N}^{(i)} \otimes \mathbf{N}^{(i)} = \mathbf{N}^{(i)} \cdot \boldsymbol{\varepsilon}\mathbf{N}^{(i)}$. Then a least-squares algorithm is formed from residuals based on (29). Although one can understand the motivation of (29), upon critical examination these kinematics are objectionable from the outset. Traditional definitions of strain tensors do not operate on planar normals, but on tangent vectors or line elements, and these have different behavior under the same transformation. For example, consider the Lagrangian strain tensor given by

$$\boldsymbol{E} = (1/2)\left(\boldsymbol{H}^{\mathrm{T}}\boldsymbol{H} - \boldsymbol{I}\right). \tag{30}$$

Noting from (8) that $\boldsymbol{H}$ operates on line elements, equation (30) indicates that $\boldsymbol{E}$ likewise operates on line elements. Instead, the appropriate kinematic relationship for planar normals is obtained from Nanson's formula (Chadwick, 1999),

$$(\det \boldsymbol{H})\boldsymbol{H}^{-\mathrm{T}}\mathbf{N}^{(i)} = \mu^{(i)}\mathbf{n}^{(i)},$$

where $\mathbf{n}^{(i)}$ is the deformed unit normal, $\mu^{(i)} = (\boldsymbol{C}^{-1} \cdot \mathbf{N}^{(i)} \otimes \mathbf{N}^{(i)})^{1/2}$ is the area ratio, and $\boldsymbol{C} \equiv \boldsymbol{H}^{\mathrm{T}}\boldsymbol{H} = \boldsymbol{U}^2$.

To be clear, we will not, in the end, seriously object to the use of (29) for small strain studies, which is the most common situation to date. We point out the deficiency should experimental conditions advance to the point where using (29) would give distinguishable errors, or for the large elastic strain cases noted in the *Introduction*. In the next section we will show that (28) reassuringly reduces to (29) upon linear approximation. We find these computations useful to elucidate, since this equivalence may not be evident upon first comparing (29) and (28).

3.2. Linear approximation procedure

We now derive the error made when replacing the general kinematics given by (28) with the approximate kinematics in (29). The linearization method shown here is less rigorous than the general approach given by Hughes & Pister (1978), but gives the same results [see also Section D of Yavari (2008) for other recent applications of linearization methods]. The result of the procedure is that the kinematics of (29) are correct to within an error of order $\boldsymbol{\varepsilon}^2$. For a rough idea of the meaning of this, let us assume we have strains of $\boldsymbol{\varepsilon} \simeq 1\% = 0.01$, with error $\Delta\boldsymbol{\varepsilon} = \boldsymbol{\varepsilon}^2 \simeq 1 \times 10^{-4}$. Then for a material with elastic modulus $E \simeq 100$ GPa, the nominal stress level would be $\sigma \simeq 1$ GPa and the error in the stress would be $\Delta\sigma \simeq 10$ MPa. This error is currently below the magnitude of errors arising from other sources such as precision uncertainty (Edmiston *et al.*, 2011); however, as instrumentation and data-analysis algorithms improve, this may not always be the case. From another perspective, at the higher stress levels which may be obtained in diamond anvil cell or shock experiments, where $\sigma \simeq 10$ GPa, this error may also be detectable.

We begin by considering, with the relative change in spacing for a given lattice plane, the right-hand side of (29),

$$\frac{\delta d}{d_0} = \frac{d - d_0}{d_0}. \tag{31}$$

In (31) and all the following equations, the superscript (i) designating the lattice plane will be suppressed to clean the notation. Next we employ the finite deformation kinematics of (28) to linearize (31) about the reference state. We have the typical requirements of $\boldsymbol{R} = \boldsymbol{I}$, and use a simple expansion for the stretch,

$$\boldsymbol{U} = \boldsymbol{I} + \boldsymbol{\varepsilon}. \tag{32}$$

In practice we obtain $\boldsymbol{R} = \boldsymbol{I}$ by effectively rotating the reference configuration κ. To compute $\delta d/d_0$ from (31) we expand the planar spacing in the deformed configuration, d, giving

$$d = d_0 + \left.\frac{\partial d}{\partial \varepsilon}\right|_{\varepsilon=0} \cdot \boldsymbol{\varepsilon} + O(\boldsymbol{\varepsilon}^2). \tag{33}$$

Using (33) in (31) gives the leading order expansion for the relative change in spacing as

$$\frac{\delta d}{d_0} = d_0^{-1}\left.\frac{\partial d}{\partial \varepsilon}\right|_{\varepsilon=0} \cdot \boldsymbol{\varepsilon} + O(\boldsymbol{\varepsilon}^2). \tag{34}$$

Next, it can be shown that lattice planar spacing d is related to the magnitude of a reciprocal-lattice vector $\mathbf{g}^*$ by the equation

$$(d)^{-1} = |\mathbf{g}^*|. \tag{35}$$

Substitution of (28) into (35) gives

$$d = |\mathbf{g}^*|^{-1} = \left(\boldsymbol{H}^{-\mathrm{T}}\mathbf{G}^* \cdot \boldsymbol{H}^{-\mathrm{T}}\mathbf{G}\right)^{-1/2} = \left(\boldsymbol{C}^{-1} \cdot \mathbf{G}^* \otimes \mathbf{G}^*\right)^{-1/2}. \tag{36}$$

For later use we note that in the reference state similar computations give $d_0 = |\mathbf{G}^*|^{-1}$. Then using (36) with the chain rule we compute

$$\frac{\partial d}{\partial \varepsilon_{kl}} = -\left(\frac{1}{2}\right)\frac{1}{(\boldsymbol{C}^{-1} \cdot \mathbf{G}^* \otimes \mathbf{G}^*)^{3/2}}\left[\frac{\partial (\boldsymbol{C}^{-1})_{mn} G_m^* G_n^*}{\partial \varepsilon_{kl}}\right], \tag{37}$$

where $G_m^* \equiv \mathbf{G}^* \cdot \mathbf{e}_m$ is notation for projection on the Cartesian basis. Similarly $(\boldsymbol{C}^{-1})_{mn} = \boldsymbol{C}^{-1} \cdot \mathbf{e}_m \otimes \mathbf{e}_n$. Next, we use $\boldsymbol{C} = \boldsymbol{U}^2$, the initial expansion for the stretch in (32), and the result $(\boldsymbol{I} + \boldsymbol{\varepsilon})^{-1} = \boldsymbol{I} - \boldsymbol{\varepsilon} + O(\boldsymbol{\varepsilon}^2)$ (Liu, 2002, p. 261), giving

$$\boldsymbol{C}^{-1} = \boldsymbol{I} - 2\boldsymbol{\varepsilon} + O(\boldsymbol{\varepsilon}^2). \tag{38}$$

Then substitution of (38) into (37) and evaluating at $\boldsymbol{\varepsilon} = 0$ so that $\boldsymbol{C} \simeq \boldsymbol{I}$ gives

$$\left.\frac{\partial d}{\partial \varepsilon_{kl}}\right|_{\boldsymbol{\varepsilon}=\mathbf{0}} = \frac{1}{(|\mathbf{G}^*|)^3} G_k^* G_l^*. \tag{39}$$

Now we write $\mathbf{G}^* = |\mathbf{G}^*|\hat{\mathbf{G}}^*$ where $\hat{\mathbf{G}}^*$ is the unit vector associated with $\mathbf{G}^*$. The properties of reciprocal-space geometry are such that $\hat{\mathbf{G}}^* = \mathbf{N}$, where $\mathbf{N}$ is the unit normal to the lattice plane. Using this property, (39) and $d_0 = |\mathbf{G}^*|^{-1}$ in (34) give, after simplifications,

$$\frac{\delta d}{d_0} = \boldsymbol{\varepsilon} \cdot \mathbf{N} \otimes \mathbf{N} + O(\boldsymbol{\varepsilon}^2). \tag{40}$$

So we have shown that the finite deformation expression of (28) reduces to the conventional expression of (29) upon a linearization procedure. The infinitesimal relation in (29) is therefore demonstrated to be correct to within an error of $O(\boldsymbol{\varepsilon}^2)$. The detailed form of the error term is a complicated function and is too lengthy to report here. Should there be desire to compute these higher-order terms by continuing the expansion, we suggest simply using the finite deformation framework from the beginning.

4. Conclusion

In this study we have derived the relations between the descriptions of lattice distortion based on unit-cell parameters and that based on a lattice deformation tensor relative to a fixed reference configuration, κ. This was done to establish the equivalences of the two approaches in order to assist in communications and collaborations between communities. We pointed out that the lattice deformation tensor approach should be preferred for studies where constitutive quantities such as stress tensors are eventually required. This is because the constitutive formula for phenomenological continuum theories are explicitly expressed in terms of tensor functions of $\boldsymbol{H}_\kappa$; in addition, in this framework the uncertainties for lattice stretch and rotation are naturally decoupled (Edmiston *et al.*, 2011).

We have also derived the evolution relation for reciprocal-lattice vectors under finite lattice deformations, $\boldsymbol{H}$. This result enabled the demonstration that the finite deformation relations of (28) reduce to the more commonly used infinitesimal kinematic relations of (29) upon linearization about the reference state. The error term in using the infinitesimal kinematic relations was shown to be $O(\boldsymbol{\varepsilon}^2)$. Recognition of this error when using small strain kinematics is becoming more important to consider as experimental precisions improve and as higher lattice strain levels are probed. The implementation of (28) into analysis codes is a suggested course of action to avoid this error, should there be sufficient need.

APPENDIX *A*
Derivation of Cartesian representation for unit-cell geometry

In this section we compute the details of the derivation of the structural map reported in equation (11); see also Neustadt *et al.* (1968) for an alternative approach. We pick up the development from equation (5). Recall we adopt the convention for the mapped cell edges as

$$\mathbf{a} = a\mathbf{e}_1, \quad \mathbf{b} = b\mathbf{e}_r(\gamma; \mathbf{e}_1, \mathbf{e}_2), \quad \mathbf{c} = c\hat{\mathbf{c}}(\alpha, \beta, \gamma),$$

where from the definition of the internal angles α, β we have $\hat{\mathbf{c}} \cdot \hat{\mathbf{a}} \equiv \cos\beta$, $\hat{\mathbf{c}} \cdot \hat{\mathbf{b}} \equiv \cos\alpha$. We require an expression for $\mathbf{c}$, hence $\hat{\mathbf{c}}$, on the Cartesian basis $\mathbf{e}_1$, $\mathbf{e}_2$, $\mathbf{e}_3$. To achieve this, we find it useful to consider the intermediate step of constructing a basis which is reciprocal to that defined by

$$\mathbf{h}_1 = \mathbf{e}_1, \quad \mathbf{h}_2 = \mathbf{e}_r(\gamma; \mathbf{e}_1, \mathbf{e}_2), \quad \mathbf{h}_3 = \mathbf{e}_3. \tag{41}$$

Note that $\mathbf{h}_1 = \hat{\mathbf{a}}$ and $\mathbf{h}_2 = \hat{\mathbf{b}}$. Denote the corresponding reciprocal basis by $\mathbf{h}_i^*$. Next we make use of the result of equation (24); we can write

$$\hat{\mathbf{c}} = \boldsymbol{I}\hat{\mathbf{c}} = (\hat{\mathbf{c}} \cdot \mathbf{h}_i)\mathbf{h}_i^* = (\hat{\mathbf{c}} \cdot \mathbf{h}_i^*)\mathbf{h}_i, \tag{42}$$

relations which hold for any vector. Expanding $(42)_2$, we have the representation

$$\hat{\mathbf{c}} = (\hat{\mathbf{c}} \cdot \mathbf{h}_1)\mathbf{h}_1^* + (\hat{\mathbf{c}} \cdot \mathbf{h}_2)\mathbf{h}_2^* + (\hat{\mathbf{c}} \cdot \mathbf{h}_3)\mathbf{h}_3^* = \cos\beta\mathbf{h}_1^* + \cos\alpha\mathbf{h}_2^* + \hat{c}_3\mathbf{h}_3^*, \tag{43}$$

where we have used $\mathbf{h}_1 = \hat{\mathbf{a}}$ and $\mathbf{h}_2 = \hat{\mathbf{b}}$ along with the definition of the unit-cell angles β, α. The unknown component $\hat{c}_3$ can be obtained from the unit vector property, $|\hat{\mathbf{c}}| = 1$, which we now show. Using (43) we have

$$1 = |\hat{\mathbf{c}}|^2 = \cos^2\beta(\mathbf{h}_1 \cdot \mathbf{h}_1^*) + \cos^2\alpha(\mathbf{h}_2^* \cdot \mathbf{h}_2^*) + \hat{c}_3^2 + 2\cos\beta\cos\alpha(\mathbf{h}_1 \cdot \mathbf{h}_2), \tag{44}$$

where we have used $\mathbf{h}_1^* \cdot \mathbf{h}_3^* = \mathbf{h}_2^* \cdot \mathbf{h}_3^* = 0$, which will be justified shortly. After some algebra, we obtain

$$\hat{c}_3 = \left[1 - \cos^2\beta(\mathbf{h}_1^* \cdot \mathbf{h}_1^*) - \cos^2\alpha(\mathbf{h}_2^* \cdot \mathbf{h}_2^*) - 2\cos\beta\cos\alpha(\mathbf{h}_1^* \cdot \mathbf{h}_2^*)\right]^{1/2}. \tag{45}$$

We now construct the reciprocal basis $\mathbf{h}_i^*$ to complete the specification of $\mathbf{c}$. Using $(42)_3$ applied to $\mathbf{h}_i^*$ we have

$$\mathbf{h}_i^* = \left(\mathbf{h}_i^* \cdot \mathbf{h}_j^*\right)\mathbf{h}_j = \mathbf{h}_{ij}^*\mathbf{h}_j, \tag{46}$$

where $h_{ij}^* = \mathbf{h}_i^* \cdot \mathbf{h}_j^*$ is the reciprocal metric tensor. It is related to the metric tensor $h_{ij}^* = \mathbf{h}_i \cdot \mathbf{h}_j$ by the relation $[h_{ij}^*] = [h_{ij}]^{-1}$, where the bracket notation is used to emphasize matrix representations. To see this, use the sequence $\delta_{ik} = \mathbf{h}_i^* \cdot \mathbf{h}_k = h_{ij}^*\mathbf{h}_j \cdot \mathbf{h}_k = h_{ij}^* h_{jk}$. Then, by the uniqueness of matrix inverses, $[h_{ij}^*] \equiv [h_{ij}]^{-1}$. Next we explicitly compute the metric h_{ij} in matrix form as

$$[h_{ij}] = \begin{bmatrix} \mathbf{h}_1 \cdot \mathbf{h}_1 & \mathbf{h}_1 \cdot \mathbf{h}_2 & \mathbf{h}_1 \cdot \mathbf{h}_3 \\ \mathbf{h}_2 \cdot \mathbf{h}_1 & \mathbf{h}_2 \cdot \mathbf{h}_2 & \mathbf{h}_2 \cdot \mathbf{h}_3 \\ \mathbf{h}_3 \cdot \mathbf{h}_1 & \mathbf{h}_3 \cdot \mathbf{h}_2 & \mathbf{h}_3 \cdot \mathbf{h}_3 \end{bmatrix} = \begin{bmatrix} 1 & \cos\gamma & 0 \\ \cos\gamma & 1 & 0 \\ 0 & 0 & 1 \end{bmatrix}, \tag{47}$$

where we have used (41) and (6). The reciprocal metric h_{ij}^* is obtained by taking the matrix inverse, giving

$$[h_{ij}^*] = [h_{ij}]^{-1} = \begin{bmatrix} 1/(1-\cos^2\gamma) & -\cos\gamma/(1-\cos^2\gamma) & 0 \\ -\cos\gamma/(1-\cos^2\gamma) & 1/(1-\cos^2\gamma) & 0 \\ 0 & 0 & 1 \end{bmatrix}. \tag{48}$$

Use of the entries of (48) in (46) with (41) gives the reciprocal bases $\{\mathbf{h}_i^*\}$ as

$$\mathbf{h}_1^* = \left(\frac{1}{1-\cos^2\gamma}\right)\mathbf{e}_1 + \left(\frac{-\cos\gamma}{1-\cos^2\gamma}\right)\mathbf{e}_r(\gamma; \mathbf{e}_1, \mathbf{e}_2), \tag{49}$$

$$\mathbf{h}_2^* = \left(\frac{-\cos\gamma}{1-\cos^2\gamma}\right)\mathbf{e}_1 + \left(\frac{1}{1-\cos^2\gamma}\right)\mathbf{e}_r(\gamma; \mathbf{e}_1, \mathbf{e}_2), \tag{50}$$

$$\mathbf{h}_3^* = \mathbf{e}_3. \tag{51}$$

Now to complete (45) we require

$$\begin{aligned} \mathbf{h}_1^* \cdot \mathbf{h}_2^* = h_{12}^* &= \frac{-\cos\gamma}{1-\cos^2\gamma}, \\ \mathbf{h}_1^* \cdot \mathbf{h}_1^*, \mathbf{h}_2^* \cdot \mathbf{h}_2^* = h_{11}^*, h_{22}^* &= \frac{1}{1-\cos^2\gamma}. \end{aligned} \tag{52}$$

where we have used (48). These results simplify (45) to

$$\hat{c}_3 = \frac{1}{\sin\gamma} \times \left(1 + 2\cos\alpha\cos\beta\cos\gamma - \cos^2\alpha - \cos^2\beta - \cos^2\gamma\right)^{1/2}. \tag{53}$$

Finally, we have

$$\mathbf{c} = c\hat{\mathbf{c}} = c\cos\beta\mathbf{h}_1^* + c\cos\alpha\mathbf{h}_2^* + c\hat{c}_3\mathbf{h}_3^*, \tag{54}$$

where $\hat{c}_3$ is given by (53).

We are now able to compute $\boldsymbol{H}_\mathrm{s}$ from (10). Recall that

$$\boldsymbol{H}_\mathrm{s} = \mathbf{a} \otimes \mathbf{e}_1 + \mathbf{b} \otimes \mathbf{e}_2 + \mathbf{c} \otimes \mathbf{e}_3.$$

We compute the matrix representation of $\boldsymbol{H}_\mathrm{s}$ from $H_{ij} = \mathbf{e}_i \cdot \boldsymbol{H}_\mathrm{s}\mathbf{e}_j$ by using (49)–(51) in equation (54), along with equations (3), (4) and (6). We obtain

$$\boldsymbol{H}_\mathrm{s} = \begin{bmatrix} a & b\cos\gamma & c\cos\beta \\ 0 & b\sin\gamma & c(\cos\alpha - \cos\beta\cos\gamma)/\sin\gamma \\ 0 & 0 & c(1 + 2\cos\alpha\cos\beta\cos\gamma - \cos^2\alpha - \cos^2\beta - \cos^2\gamma)^{1/2}/\sin\gamma \end{bmatrix}.$$

This matches accepted results from the literature (Bernier *et al.*, 2011).

This work was performed under the auspices of the US Department of Energy by Lawrence Livermore National Laboratory under Contract DE-AC52-07NA27344 (LLNL-JRNL-507832). JE is supported by the Lawrence Scholar Program.

References

Adams, B. & Olson, T. (1998). *Prog. Mater. Sci.* **43**, 1–88.
Azaroff, L., Kaplow, R., Kato, N., Weiss, R., Wilson, A. & Young, R. (1974). *X-ray Diffraction.* New York: McGraw-Hill.
Bernier, J. V., Barton, N. R., Lienert, U. & Miller, M. P. (2011). *J. Strain Anal. Eng. Des.* **46**, 527–547.
Callister, W. D. (2000). *Materials Science and Engineering*, 5th ed. New York: John Wiley and Sons.
Chadwick, P. (1999). *Continuum Mechanics: Concise Theory and Problems.* New York: Dover.
Cullity, B. (1978). *Elements of X-ray Diffraction.* Reading: Addison-Wesley.
Edmiston, J. K., Barton, N. R., Bernier, J. V., Johnson, G. C. & Steigmann, D. J. (2011). *J. Appl. Cryst.* **44**, 299–312.
Efstathiou, C., Boyce, D., Park, J.-S., Lienert, U., Dawson, P. & Miller, M. (2010). *Acta Mater.* **58**, 5806–5819.
Guiner, A. (1963). *X-ray Diffraction.* London: W. H. Freeman.
Gupta, A., Steigmann, D. & Stolken, J. (2011). *J. Elast.* **104**, 249–266.
Hawreliak, J., El-Dasher, B., Lerenzana, H., Kimminau, G., Higginbotham, A., Vinko, S., Murphy, W., Rothman, S. & Park, N. (2011). *Phys. Rev. B*, **83**, 144144.
Hughes, T. J. & Pister, K. S. (1978). *Comput. Struct.* **8**, 391–397.
Jayaraman, A. (1983). *Rev. Mod. Phys.* **55**, 65–108.
Kalantar, D. *et al.* (2005). *Phys. Rev. Lett.* **95**, 075502.
Katrusiak, A. (2008). *Acta Cryst.* A**64**, 135–148.
Liu, I.-S. (2002). *Continuum Mechanics.* Berlin/Heidelberg: Springer-Verlag.
Mach, J. C., Beaudoin, A. J. & Acharya, A. (2010). *J. Mech. Phys. Solids*, **58**, 105–128.
Miller, M., Park, J., Dawson, P. & Han, T. (2008). *Acta Mater.* **56**, 3927–3939.
Neustadt, R. J., Cagle, F. W. & Waser, J. (1968). *Acta Cryst.* A**24**, 247–248.
Noyan, I. & Cohen, J. (1987). *Residual Stress: Measurement by Diffraction and Interpretation.* New York: Springer-Verlag.
Winther, G., Margulies, L., Schmidt, S. & Poulsen, H. (2004). *Acta Mater.* **52**, 2863–2872.
Yamanaka, T., Fukuda, T., Hattori, T. & Sumiya, H. (2001). *Rev. Sci. Instrum.* **72**, 1458–1462.
Yavari, A. (2008). *J. Math. Phys.* **49**, 022901.